25th ABCM International Congress of Mechanical Engineering
October 20-25, 2019, Uberlândia, MG, Brazil

COB-2019-1660
HEAT EMITTER FOR PLUG AND ABANDONMENT OF OIL WELLS

Rafael Adriano Alves Camargo Gonçalves
Igor Alves de Carvalho
Marcelo J. S. de Lemos
Instituto Tecnológico de Aeronáutica, 12228-900, São José dos Campos/SP – Brasil
rafaelacamagon@gmail.com
carvalho.iadc@gmail.com
delemos@ita.br

Abstract. *Demand for decommissioning of matured oil fields worldwide has motivated a Plug & Abandonment "wave" that has driven the development of new and disruptive technologies. This work numerically investigates the effect of thermal emitter inside a well, which has the purpose of sealing abandoned wells. The variation of two parameters are studied: heat generation rate and emitter length. The mathematical model involves flow and energy equations, which are discretized using the control volume method and solved by a segregated algorithm. The results indicate that for the cases here tested, both parameters are important to the thermal mechanism. The heat generation rate determines the maximum temperature and cooling time. The emitter length also influences the cooling time and the area of thermal affected zone.*

Keywords: *plug and abandonment, decommissioning, heat emitter.*

1. INTRODUCTION

Petroleum products are present in a wide range of different forms in people's lives, from school supplies to fuels. Until today, some businessmen from different countries have explored and extracted oil in deep water, which has increased the world's oil supply (Vralstrad, 2019). The exploration in deep water needs more investment and effort than onshore exploration (Barclay et al., 2001), what usually results in bigger cost. In addition to exploration cost, there are production costs and well abandonment costs that can be seen as an indirect cost, once it normally appears at the final stage of an oil well, when there is no more viable oil to be extracted or when the well has some integrity issue. This cost represents a big passive that is increasing day by day, since some wells explored on the last decades are coming to their ends (Barclay et al., 2001). The cost reduction due to new technologies are becoming necessary (Khalifeh et al., 2013).

The common name of well abandonment process is Plug and Abandonment (P&A). Normally, the operation consists of filling a portion of the well with cement, obstructing the oil flow through different geological structures (Vralstrad et al., 2019). This method has been applied on several wells. Unfortunately, the operation cost is extremely high, especially when the operation occurs in deep water. One reason behind the big cost is the time of each required process in P&A operations, especially the time spent to remove the production tubing. One recent unexplored alternative method is to apply a heat emitter, such as thermite, into the well to melt several well elements (pipes, casing and cement), creating a solid and impermeable plug (Vralstrad et al., 2019). The heat emitter method has a huge potential to change disruptively the P&A operations.

As the abandonment phase entails huge costs, companies try to extend the life of an oil and gas extraction field for as long as possible through a combination of efficiency improvements and cost reduction methods. Every decommissioning project has a multidisciplinary approach focused on evaluating all feasible abandonment, risk and cost options. This is key to creating a collaborative environment by interacting with different stakeholders, partners and regulatory agencies during the planning and execution phases of abandonment. The definition of the decommissioning approach to be used is typically a balance between regulatory requirement, environmental impact, energy use, gaseous emissions, technical feasibility, cost, social impact, public opinion, health and safety.

Field trials of new equipment for the exploration and production of offshore oil occur in complex conditions on the seabed, and at long distances from the sea coast, which intensify the difficulties in the technological development of equipment and systems for oil activities at sea. The decommissioning industry is increasing worldwide and companies focused on developing a specialization in this complex and multidisciplinary area will be able to make the most of this significant economic opportunity.

Thermal analysis of the heat emitter and its behavior in the environment is extremely important to produce a correct plug and abandonment operation. The present study aims to analyze the thermal behavior of a well plugging operation

on pre-salt oil wells, using thermite as the heat emitter. An illustration of the current study is shown in Fig 1. The thermite is positioned inside the oil production casing, in the caprock formation, between two thermal barriers.

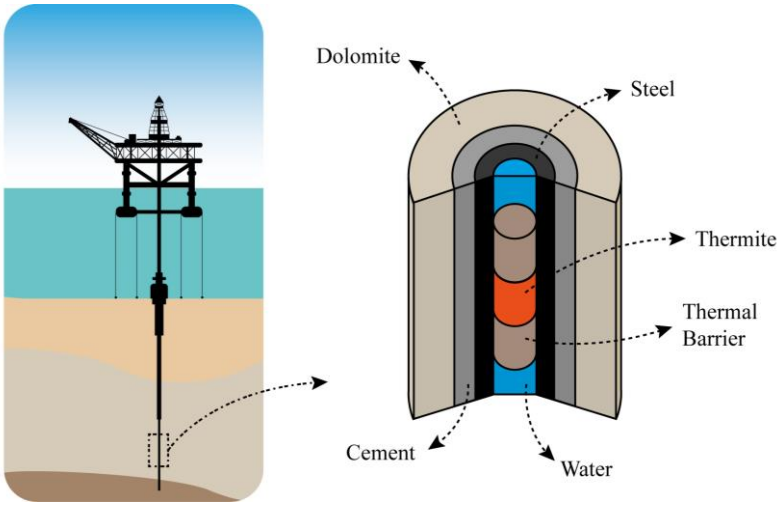

Figure 1. Case illustration (out of scale).

2. METODOLOGY

The main function of heat emitter in P&A is the melting of several well elements (production column, production casing, cement and the caprock) in certain regions. Parameters such as the heat emitter geometry and its volumetric heat generation, besides materials properties, are important aspects in well sealing process. The present study consisted of thermal analysis on the influence of two important factors: emitter length and volumetric heat generation. Other parameters, such as pipe diameters and thermal material properties, are considered constant. The Table 1 informs some physicals properties of water, thermite (Brito et al., 2005), steel API X80 (Chunyan et al., 2014), cement (Xu et al., 2000) and dolomite (Eppelbaum et al., 2014) used in this study. The thermal barrier is considered an ideal thermal isolator.

Table 1. Materials properties.

Material	Density (kg/m^3)	Specific heat (J/kg °C)	Conductivity (W/m °C)
Water	983	4185.0	0.65
Thermite	4142	748.1	47.88
API X80	7800	448.0	54.21
Cement	2010	736.0	0.53
Dolomite	2630	953.0	3.34

The emitter length analysis was done by means of 7 cases with different lengths (0.3, 0.5, 0.7, 0.9, 1.1, 1.3 and 1.5 m), all with heat generation of 30 MW/m^3. The analysis of volumetric heat generation was done by means of 7 cases with different volumetric heat generations (15, 20, 25, 30, 35, 40 and 45 MW/m^3), all with emitter of 0.9 m in length. Looking for initial results, were adopted some simplifying hypotheses: uniform heat generation along the space, constant materials properties and absence of phase change. The computational experiment was performed using the GENC-PorMed software, which in turn uses the finite volume method to discretize all the equations, implicitly solving the variables for each step of time. The mathematical models of mass conservation, momentum and energy, for porous media (de Lemos, 2012), are presented below:

$$\nabla \cdot \mathbf{u}_D = 0 \tag{1}$$

$$\rho\left[\frac{\partial \mathbf{u}_D}{\partial t} + \nabla \cdot \frac{\mathbf{u}_D \mathbf{u}_D}{\phi}\right] = -\nabla \phi \langle p \rangle^i + \mu \nabla^2 \mathbf{u}_D - \rho g \phi\left[\beta_\phi\left(\langle T \rangle^i - T_{ref}\right)\right] - \left[\frac{\mu \phi}{K}\mathbf{u}_D + \frac{C_F \phi \rho}{\sqrt{K}}|\mathbf{u}_D|\mathbf{u}_D\right] \tag{2}$$

$$\left[\left(\rho c_p\right)_f \phi + \left(\rho c_p\right)_s (1-\phi)\right]\frac{\partial \langle T\rangle^i}{\partial t}(\rho c_p)_f \nabla\cdot(\mathbf{u}_D \langle T\rangle^i) = \nabla\cdot\left[\mathbf{K}_{eff}\cdot\nabla\langle T\rangle^i\right] \quad (3)$$

where $\boldsymbol{u_D}$ is the velocity vector of Darcy, where by the Dupuit-Forchheimer relation $\boldsymbol{u_D} = \phi <\boldsymbol{u}>^i$, Φ is he medium porosity, ρ is the density, $<p>^i$ is the mean static pressure, μ is the dynamic viscosity, $\boldsymbol{g}$ is the gravity acceleration vector, $<T>^i$ is the mean temperature, T_{ref} is a reference temperature, K is the medium permeability, C_F is the drag coefficient, c_p is the specific heat of the fluid (f) and the solid (s), and $\boldsymbol{K_{eff}}$ is the effective conductive tensor. Along the domain's contours were set a temperature of 60 °C (Abdelal et al., 2015), wall condition, except in the left contour, which has a condition of axissimetry applied.

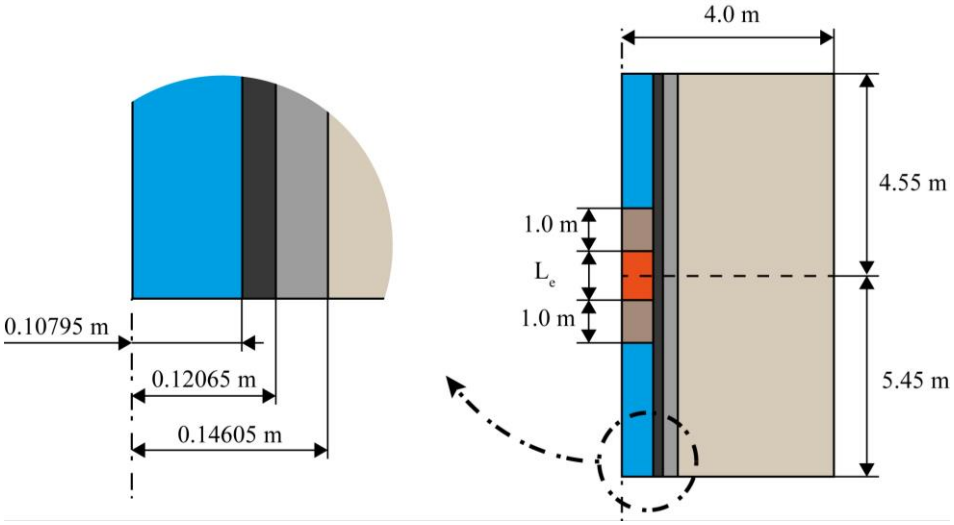

Figure 2. Case dimensions (out of scale).

3. RESULTS

A study on the influence of the grid on the results was performed. The study consisted of simulating an emitter with 0.9 m of length and 30 MW/m^3 of heat generation, only during the generation period (300 s), using five levels of mesh refining along the radial direction. The numbers of volumes along the radial direction are 50, 75, 100, 125 and 150. The number of volumes along the axial direction was set in 100. A mesh with 50 volumes along the radial direction resulted in divergence, so it was removed out from the mesh independence analyze. In order to determine the mesh's influence on results, the relative deviation of the temperature was obtained for each mesh. The exact point of data acquisition is inside the middle region of the thermite, because there is the biggest deviation on temperature from gross mesh to fine mesh. Figure 3 illustrates the relative deviation of temperature and the computational time for each mesh presented.

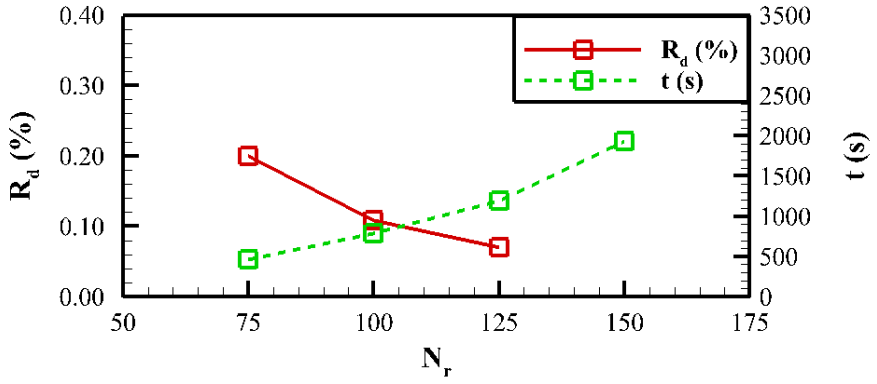

Figure 3. Relative deviation versus total number of volumes along radial direction.

where R_d(%) is the relative deviation of the temperature between the two successive meshes, N_r is the number of volumes along the radial direction and t (s) is the computational time.

The biggest relative deviation of temperature (0.20 %) was obtained using 75 volumes along radial direction (total of 7500 volumes) and has a computational time of 464.07 s related to it. The mesh with 100 volumes along radial and axial direction (total of 10000 volumes) was selected, principally because it has small relative deviation of temperature (0.11 %) and the computational time is not prohibited (783.78 s). The discretized domain is shown in Fig. 4. The region of the water, thermite and thermal barrier column has volumes with 0.01 m wide and 0.10 m high, while the dolomite region has volumes with 0.0433 m wide and 0.1 m high.

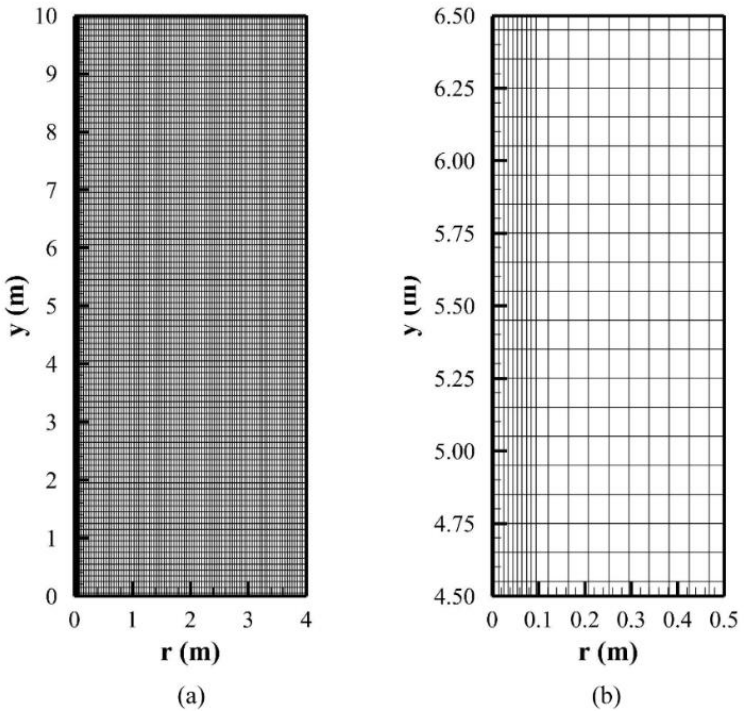

Figure 4. Discrete domain.

The heat generation capacity may be the most important parameter of a heat emitter, as well as the thermal diffusion. The study on heat generation is important to obtain an overview about the phenomenon and its response mechanisms regarding the intensity of heat generation. A study on volumetric heat generation was carried out using 7 different volumetric heat generations (15, 20, 25, 30, 35, 40 and 45 MW/m^3) and an emitter with 0.9 m of length. The higher the heat generation the higher the final temperatures. Figure 5 illustrates the radial profiles of the temperature.

The radial temperature distribution in Fig. 5, shows that cement is a huge thermal obstacle, in contrast to steel (API X80). Shortly after the end of reaction, the temperature of the outermost cement surface (75 °C for 15 MW/m^3 and 104 °C for 45 MW/m^3) has increased too little for all generation rates, once cement has diffusivity much lower than thermite and steel.

The hypothesis of homogeneous heat generation is good enough, since the generation rate is much superior to heat transfer through cement, even for real activation systems (Abdelal et al., 2015). However, the cement inner surface has huge temperature differences between the cases (891 °C for 15 MW/m^3 and 2554 °C for 45 MW/m^3), what promotes a huge heat flux through cement (17.03 and 51.12 kW/m^2 for the cases with 15 and 45 MW/m^3 of generation produced by the emitter, respectively). The intensity of those heat flux is important to understand the cement behavior, since the cement may show cracks in applications with high temperatures.

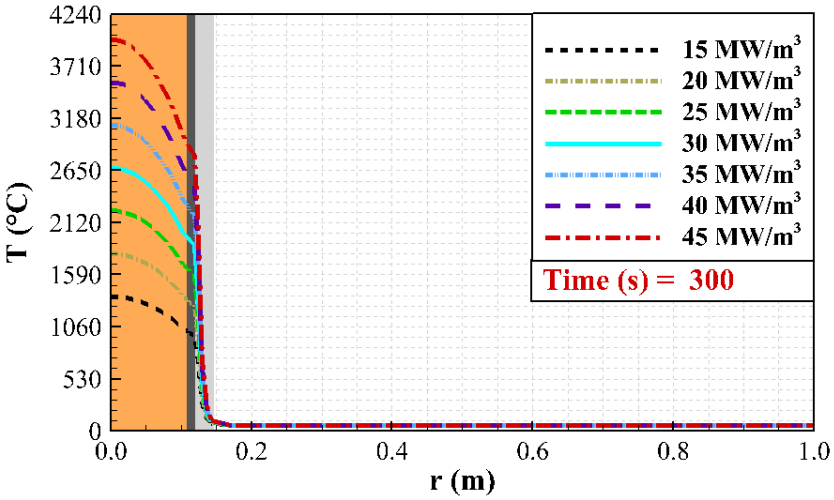

Figure 5. Radial temperature profile, at emitter central region (y = 5.45m), for heat generation analyzes in t = 300s.

After the cooling period of 4 hours, the temperature differences between cement inner and outer surface have decreased in 77.7 % for all cases, according to Fig. 6. Therefore, the heat generation magnitude does not influence the rate of reduction of the heat flow, what makes predictable the temperature difference through cement if some rate of reduction of the heat flow of a single case is known. The largest heat generations still promote the greatest temperature differences at the cement, which provides the greatest heat flows (3.82 and 11.37 kW/m^2 for the cases with 15 and 45 MW/m^3 of generation produced by the emitter, respectively). The maximum temperature for dolomite, after 4 hours of cooling, is 278 °C for 15 MW/m^3 and 715 °C for 45 MW/m^3.

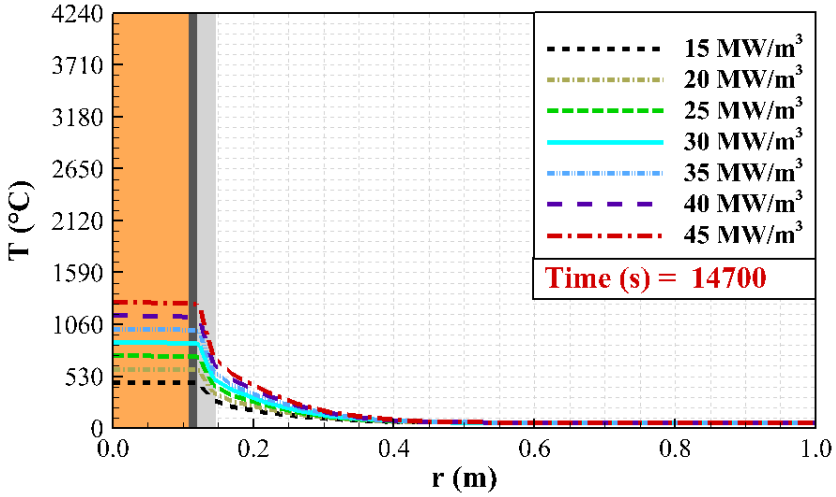

Figure 6. Radial temperature profile, at emitter central region (y = 5.45 m), for heat generation analyzes in t = 14700 s.

Disregarding the phase change, the temperature field along steel, cement and dolomite has higher temperature levels than it would have with phase change models. Meanwhile, the higher temperature field could give an extreme scenario for heat transfer. In other words, the heat penetration in the cement and dolomite is overestimated when the phase change is not considerate.

Figure 7 shows the temperature profiles, in the axial direction with r = 0.11895 m, with vertical lines to represent the emitter length (from 5.0 to 5.9 m). It was noticed that the steel vertical length with highest temperatures decrease with heat generation. The small steel thickness, which affects the radial heat flux, and cement conduction, which affects the gradient of temperature in steel, are responsible for this phenomenon. So, the emitter length must be bigger than desired thermal length (length with temperature above melting point), specially for higher heat generation rates.

During the cooling period (4 hours), the temperature profile has decreased from the center to emitter's axial extremities. This consolidates the emitter length importance to ensure a temperature profile capable of melt the steel according to the project specifications.

The temperatures profile capable of melt the steel according to the project, it is necessary to know the time in which these temperatures remain above a reference melting temperature (1500 °C) emitted by the heat emitter. Figure 9 shows the relation between the time duration that maximum temperature remains above the melting temperature (t_m) and the emitter volumetric heat generation ($\dot{Q}$). There is a nonlinear behavior, where the melt temperature curve shows a slight declination, making it clear that the increase in melt temperature t_m due to the increased volumetric heat generation of the emitter $\dot{Q}$ becomes smaller with the increase of $\dot{Q}$.

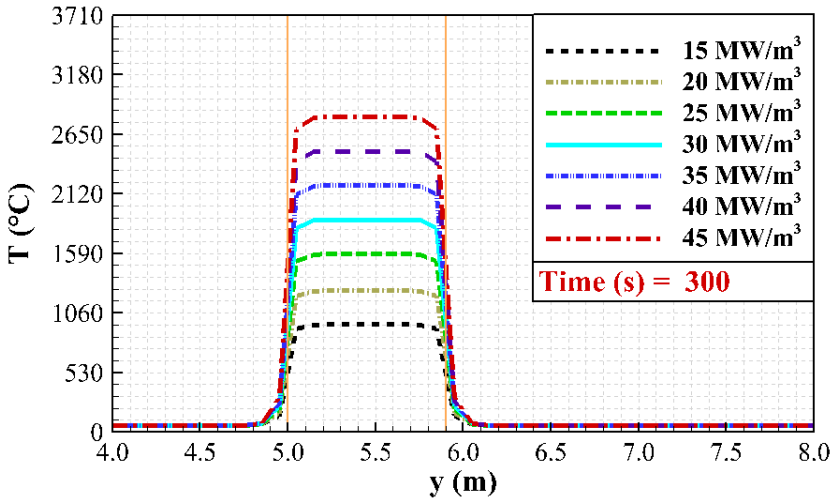

Figure 7. Axial temperature profile, at steel outermost surface (r = 0.11895 m), for heat generation analyzes in t = 300 s.

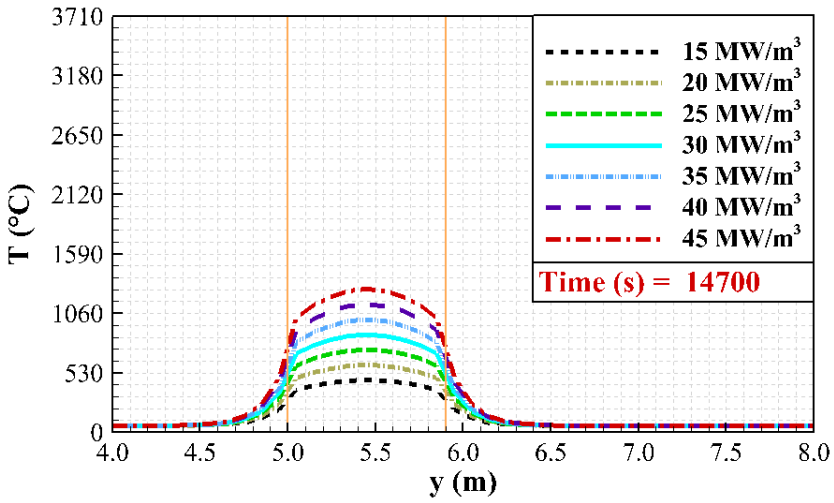

Figure 8. Axial temperature profile, at steel outermost surface (r = 0.12065 m), for heat generation analyzes in t = 14700 s.

The phenomenon can be visualized by means of the combination of two distinct mechanisms: increase of the internal energy and increase of the thermal flux on the outermost steel surface. Firstly, the increase of heat generation promotes the increase of the steel internal energy, which would result in the increase of maximum temperatures and the melting temperature t_m. Secondly, the heat flux increases according to the increase of maximum temperatures, which tends to decrease the melting temperature t_m.

As important as heat generation and propagation, emitter length is a crucial parameter and its effects on the thermal mechanism in well abandonment need to be analyzed. A study on emitter length was performed using 7 different lengths (0.3, 0.5, 0.7, 0.9, 1.1, 1.3 and 1.5 m) with 30 MW/m^3 of heat generation. Differently the observed study on the influence of volumetric heat generation, the emitter length does not appear to change the final reaction temperatures along the emitter (t = 300 s), since all emitters have the same specific heat, density and heat generation. Figure 10 shows the radial temperature profiles in the considered times.

The heat generation from heat emitters is much faster than energy transport to other materials that make up the well structure. Therefore, temperature profiles need specific time to have different profiles after 4 hours of cooling, as can be seen in Fig. 11. The temperature lines for each heat emitter length have definite differences, as different lengths imply different thermal capacities.

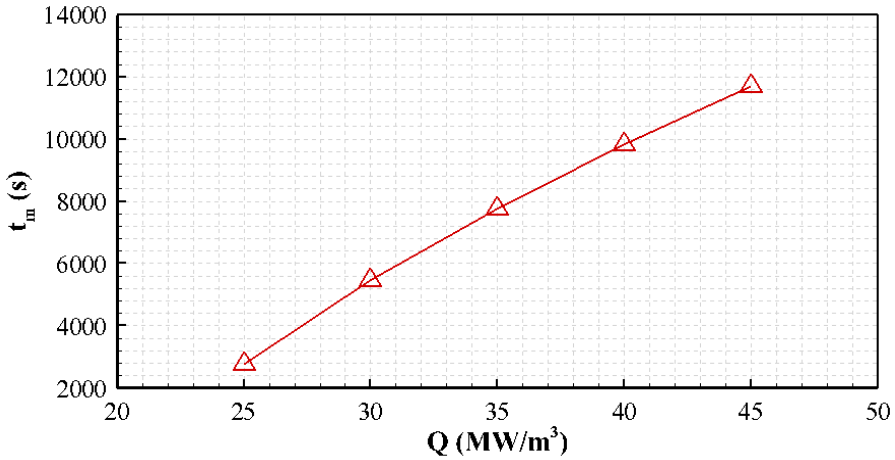

Figure 9. Time duration that temperature remains above 1500 °C (t_m) versus heat generation rate ($\dot{Q}$).

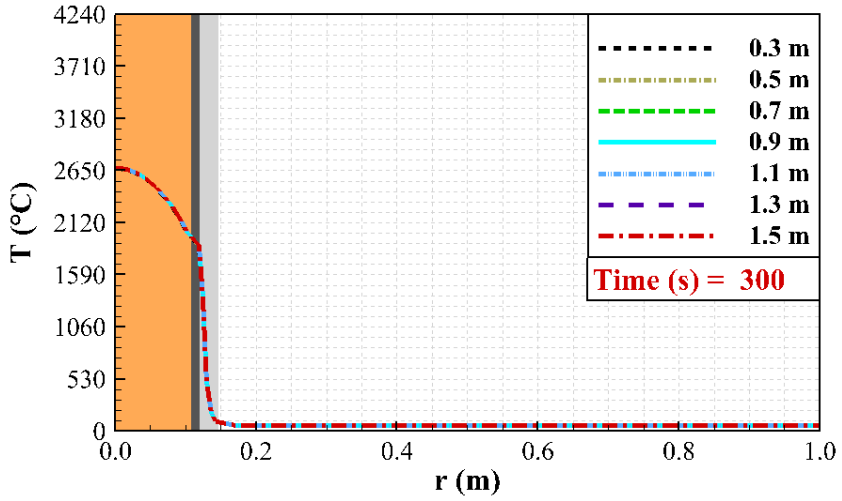

Figure 10. Radial temperature profile, at emitter central region (y = 5.45 m), for emitter length analyzes in t = 300s.

Thus, heat emitters with reduced length store less energy, which provides a shorter cooling time and a more aggressive reduction of heat flux, over time, from emitter to others well elements. The largest length promotes the greatest temperature differences at the cement (y = 5.45 m), which provides the greatest heat flows (2.78 and 9.5 kW/m^2 for the cases with 0.3 and 1.5 m of emitter length, respectively). The maximum temperature of caprock (dolomite), after 4 hours of cooling, is 291 °C for 0.3 m and 556 °C for 1.5 m.

The steel temperature profile in the end of the emitter reaction (t = 300 s) is illustrated in Fig. 12. Over again, the maximum temperatures for each emitter length do not differ from each other, since the emitter has the same maximum temperature for all analyzed lengths. After 4 hours of cooling, the temperature profiles differ, as can be seen in Fig 13. This phenomenon is due to different thermal capacities related to the difference in emitter's length.

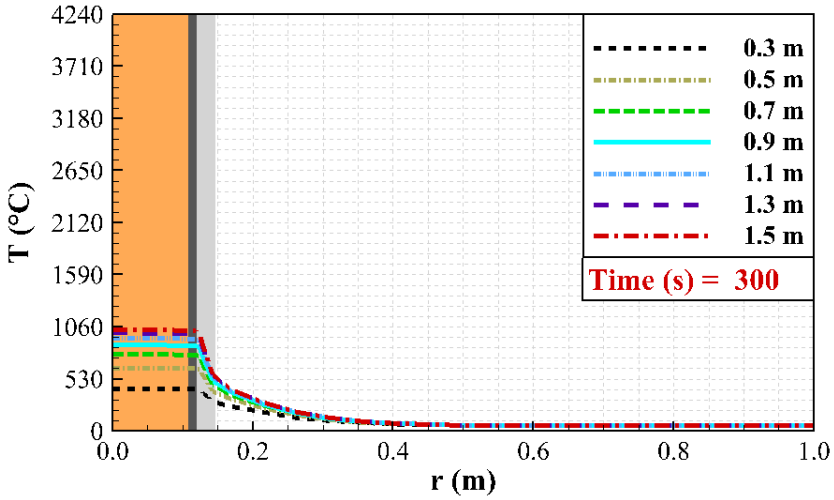

Figure 11. Radial temperature profile, at emitter central region (y = 5.45 m), for emitter length analyzes in t = 14700 s.

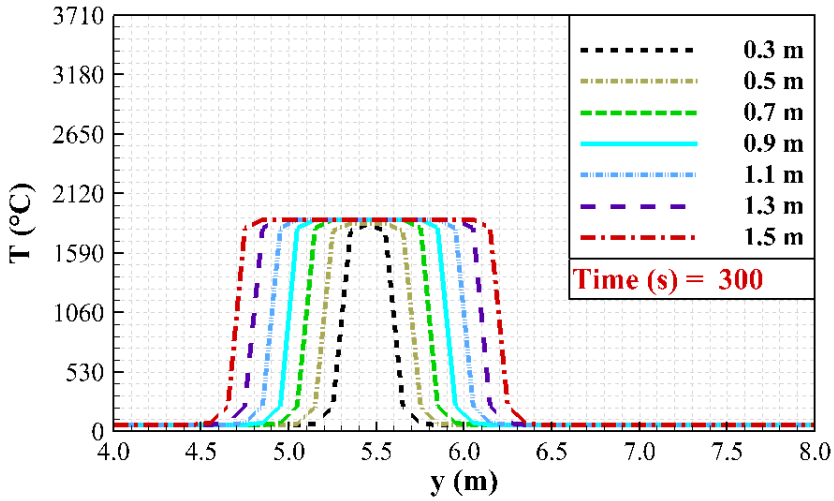

Figure 12. Axial temperature profile, at steel outermost surface (r = 0.12065 m), for emitter length analysis in t = 300 s.

The length of the heat emitter promotes an increase in the thermal capacity of the emitter, resulting in an increase in t_m. However, increasing length also results in increased heat exchange area, helping to decrease t_m. Figure 14 illustrates the variation of tm steel melting temperature with heat emitter length. A priori, thermal exchange area relevance, related to the length of the emitter, becomes larger according to the increase of the emitter length, as can be seen by the variation of the derivative of the curve shown by Fig. 14.

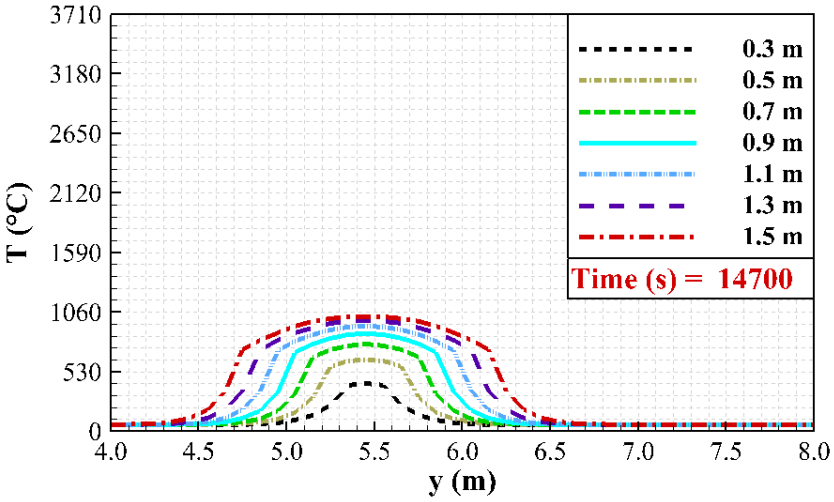

Figure 13. Axial temperature profile, at steel outermost surface (r = 0.12065 m), for emitter length analysis in t = 14700 s.

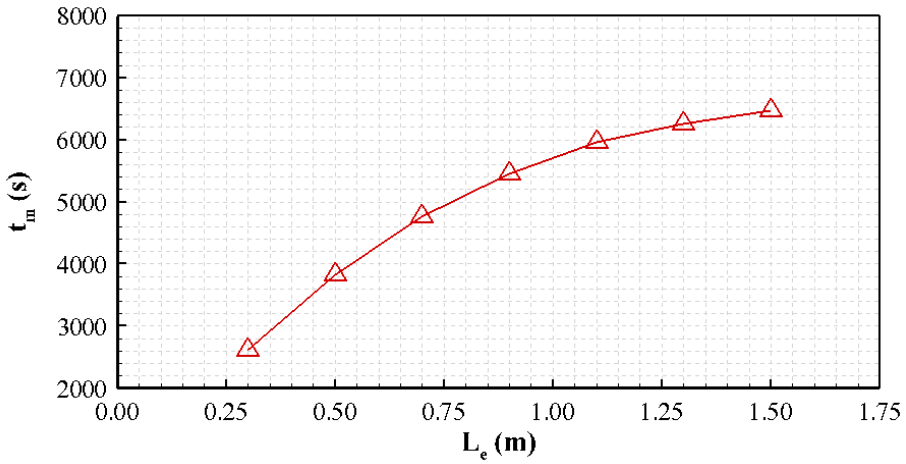

Figure 14. Time duration that temperature remains above 1500 °C (t_m) versus emitter length (L_e).

4. CONCLUSION

In the present study, the thermal behavior of a thermite-based heat emitter, for offshore well P&A, was analyzed. The influence of the heat generation rate (15, 20, 25, 30, 35, 40 and 45 MW/m^3) and the emitter lengths (0.3, 0.5, 0.7, 0.9, 1.1, 1.3 and 1.5 m) on the thermal mechanism were studied.

The results showed that increasing the volumetric heat generation increases both the steel and cement temperatures. The time that such temperatures remain above a certain reference temperature (1500 °C for steel) also increases according to the increasing the volumetric heat generation. However, the axial temperature profile along the steel is affected negatively with the generation increasing. The thermally affected length, along vertical direction in steel, decreases with increasing generation rate, causing higher emitter lengths for higher heat generation rates, which will also increase the total cooling time.

The emitter length influences the cooling time and the vertical length of the thermally affected region. Longer lengths promote larger thermally affected zones and longer cooling times due to higher internal energy values.

The study showed that the cement represents a thermal barrier and it is therefore an impediment to the formation of the plug. In this way, the optimization of the heat generation rate and the thermal transfer mechanisms must be performed. Seeking greater fidelity to the studied physical phenomena, future works should consider the variation of physical properties, such as the phase changes of the materials that make up the production tube; among them the cement and the underwater caprock.

5. ACKNOWLEDGEMENTS

This study was financed in part by the Coordenação de Aperfeiçoamento de Pessoal de Nível Superior – Brasil (CAPES) – Finance Code 001

6. REFERENCES

Abdelal, G. F., Robotham, A. and Carragher, P., 2015. "Numerical simulation of a patent technoloy for sealing of deep-sea oil wells using nonlinear finite element method". *Journal of Petroleum Science and Engineering*, Vol. 133, pp. 192-200.

Barclay, I., Pellenbarg, J., Tettero, F., Pfeiffer, J., Slater, H., Staal, T., Stiles, D., Tilling, G. and Whitney, C., 2001. "The beginning of the end: a review of abandonment and decommissioning practices". *Oilfield Review*, Vol. 13, pp. 28-44.

Brito, P., Durães, L., Campos, J. And Portugal, A., 2007. "Simulation of Fe3O3/Al combustion: Sensitivity analysys". *Chemical Engineering Science*, Vol. 62, pp. 5078-5083.

Chunyan, Y., Cuiying, L. and Bo, Y., 2014. "3D modeling of the hydrogen distribution in X80 pipeline steel welded joints". *Computational Materials Science*, Vol. 83, pp. 158-163.

Eppelbaum, L., Kutasov, I., and Pilchin, A., 2014. "Thermal properties of rocks and density of fluids". *In Applied geothermics*. Springer, Berlin, pp. 99-149.

Khalifeh, M., Hodne, H., Saasen, A. and Vralstad, T., 2013. "Techniques and Materials for North Sea Plug and Abandonment Operations". 10.4043/23915-MS. Conference: Offshore Technology Conference, At Houston, Texas, USA

Vrålstad, T., Saasen, A., Fjær, E., Øia, T., Ytrehus, J. D. and Khalifeh, M., 2019. "Plug & abandonment of offshore wells: Ensuring long-term well integrity and cost-efficiency". *Journal of Petroleum Science and Engineering*, Vol. 173, pp. 478-491.

Xu, Y. and Chung, D. D. L., 2000. "Effect of sand addition on the specific heat and thermal conductivity of cement". Cement and Concrete Research, Vol. 30, pp. 59-61

7. RESPONSIBILITY NOTICE

The authors are the only responsible for the printed material included in this paper.